



HAL
open science

Role of the Templating Heteroatom on Both Structural and Magnetic Properties of POM-Based SIM Lanthanoid Complexes

Walter Canon-Mancisidor, Gabriela Paredes-Castillo, Patricio Hermosilla-Ibanez, Diego Venegas-Yazigi, Olivier Cador, Boris Le Guennic, Fabrice Pointillart

► To cite this version:

Walter Canon-Mancisidor, Gabriela Paredes-Castillo, Patricio Hermosilla-Ibanez, Diego Venegas-Yazigi, Olivier Cador, et al.. Role of the Templating Heteroatom on Both Structural and Magnetic Properties of POM-Based SIM Lanthanoid Complexes. *European Journal of Inorganic Chemistry*, 2021, 2021 (45), pp.4596-4609. 10.1002/ejic.202100670 . hal-03414084

HAL Id: hal-03414084

<https://hal.science/hal-03414084>

Submitted on 10 Nov 2021

HAL is a multi-disciplinary open access archive for the deposit and dissemination of scientific research documents, whether they are published or not. The documents may come from teaching and research institutions in France or abroad, or from public or private research centers.

L'archive ouverte pluridisciplinaire **HAL**, est destinée au dépôt et à la diffusion de documents scientifiques de niveau recherche, publiés ou non, émanant des établissements d'enseignement et de recherche français ou étrangers, des laboratoires publics ou privés.



Distributed under a Creative Commons Attribution - NonCommercial 4.0 International License

MINIREVIEW

Role of the templating heteroatom on both structural and magnetic properties of POM-based SIM lanthanoids complexes.

Walter Cañón-Mancisidor^{*[a],[b]}, Gabriela Paredes-Castillo^{[b],[c]}, Patricio Hermosilla-Ibáñez^{[b],[c]}, Diego Venegas-Yazigi^{[b],[c]}, Olivier Cador^{*[d]}, Boris Le Guennic^[d], Fabrice Pointillart^[d].

[a] Dr. W. Cañón-Mancisidor
Mathematical and Engineering Sciences Department
Faculty of Engineering, Sciences and Technology, University Bernardo O'Higgins (UBO)
Av. Viel 1497, 8370993, Santiago de Chile, Chile.
E-mail: walter.canon@ubo.cl

[b] G. Paredes-Castillo, Dr. W. Cañón-Mancisidor, Dr. P. Hermosilla-Ibáñez, Prof. Dr. D. Venegas-Yazigi
Center for the Development of Nanoscience and Nanotechnology (CEDENNA)
University of Santiago of Chile (USACH)
Av. Libertador Bdo. O'Higgins 3363, 9170022, Santiago de Chile, Chile.

[c] G. Paredes-Castillo, Dr. P. Hermosilla-Ibáñez, Prof. Dr. D. Venegas-Yazigi
Materials Chemistry Department
Faculty of Chemistry and Biology, University of Santiago of Chile (USACH)
Av. Libertador Bdo. O'Higgins 3363, 9170022, Santiago de Chile, Chile.

[d] Prof. Dr. O. Cador, Dr. B. Le Guennic, Dr. F. Pointillart.
Univ Rennes, CNRS
ISCR (Institut des Sciences Chimiques de Rennes) - UMR 6226
F-35000 Rennes, France.

Supporting information for this article is given via a link at the end of the document

Abstract: The plasticity of the coordination chemistry of Lanthanoid ions (Ln^{III}) has allowed the design of novel coordination compounds with slow relaxation of the magnetization since the first Single Ion Magnet (SIMs) was reported by Ishikawa, who used the phthalocyaninate (Pc^{2-}) ligand to make a "sandwich type" complex. The coordination chemistry has allowed the possibility to design different types of molecular complexes with SIMs behaviour based on organic ligands. There is also SIMs based on inorganic ligands, using different types of lacunary polyoxometalates (LPOM) like, $[\text{XW}_{11}\text{O}_{39}]^{n-}$. The combination of both types of ligands can produce hybrid inorganic-organic Ln^{III} complexes with SIM behaviour. This is an attractive approach since these hybrid materials could benefit from the combination of the ease of functionalization of the organic ligands with the robustness of the inorganic moieties. There are reports that a hybrid mononuclear Dy^{III} complex could improve the relaxation dynamics when it is compared to the inorganic analogues. Thus, in this review we present a study and comparison on the improvement that inorganic and organic ligands can cause to the geometry of the metal centres of fully inorganic and hybrid (mononuclear and dinuclear) lanthanoid complexes (for Dy^{III} , Er^{III} and Yb^{III}). Moreover, we will discuss which of these changes can modify the magnetic properties of the lanthanoid complexes.

1. Introduction

In the search of new materials with new properties, the bottom-up approach enables the possibility of synthesizing by choice new molecular materials with properties such as optical, magnetic, catalytic, to mention some of them. Due to these properties several applications have been developed to fabricate the precursors of Light Emission Devices, Solar Cells, Spintronic Devices, Quantum Computing, etc. The origin of these properties relies on the electron, as stated by Verdager et al. ^[1] in the book; "Electron in Molecules", the different properties observed in molecular materials have their origin in how the electron behave; if they are localized, hopping, or excited, and if we have control on these properties we can design new materials that can be used as an alternative or complement to bulk materials.

Lanthanoid (Ln^{III}) coordination compounds almost do not have covalent character, due to the shielding of the electrons of the f orbitals by the external $5s$ and $5p$ orbitals causing that these

orbitals are the ones that participate in the bonding with the ligands. This means that the ligand defines the coordination and symmetry of the complex, so the combination of different types of ligands should have an effect on the geometry that the Ln^{III} ion will adopt^[2,3]. Ln^{III} complexes usually formed compounds with high coordination number with weak metal-ligand bonds. In the literature it is possible to find systems in which the coordination number varying from 6 to 12. This results in a great variety of coordination geometries, many of them irregular^[4,5]. For example, for an eight coordinated system, thirteen different types of geometries could be defined, however, the three most common are the square antiprism (SAPR), triangular dodecahedron (TDD) and bicapped trigonal prism (BTPR).

In the development of new magnetic materials, molecular magnets such as Single Ion Magnets based on Ln^{III} ions (Ln^{III} -SIMs)^[6-11], correspond to the second generation of Single Molecules Magnets (SMM)^[12-14], in which the main characteristic of both systems is that they can retain their magnetization over time. At low temperatures, Ln -SIMs present many physical properties such as, slow magnetic relaxation due to the anisotropy, inducing an energy barrier of the magnetization, magnetic hysteresis and quantum phenomena (Quantum Tunnelling of the Magnetization, QTM)^[12,15,16].

MINIREVIEW

Walter Cañón-Mancisidor is Associated Professor at the Universidad Bernardo O'Higgins and researcher of the Centre for Development of Nanoscience and Nanotechnology (CEDENNA), Chile. His research focusses mainly on the coordination chemistry of lanthanoid systems with magnetic or optical properties with the possibility of using these systems as building blocks for the fabrication of molecular materials.



Boris Le Guennic is Senior CNRS researcher of the Institut des Sciences Chimiques de Rennes (University of Rennes, France). His research is devoted mainly to the application of quantum chemical methodologies for the interpretation of magnetic and optical properties of transition metal and *f*-element complexes, with a particular emphasis on lanthanide-based Single Molecule Magnets.



Olivier Cadot is full Professor of the Institut des Sciences Chimiques de Rennes (University of Rennes, France) focused his research on the aim was at first to develop the synergy between electronic properties, such as magnetism and electrical conductivity, in new molecular edifices based on organic/inorganic networks. He orients now its research field to Single Molecule Magnets (SMMs) based on lanthanide.



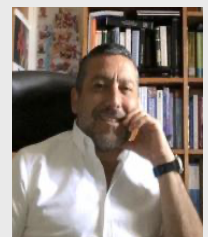
Fabrice Pointillart is a CNRS (Centre National de la Recherche Scientifique) researcher at University of Rennes 1, France. His current research interests are focused on single-molecule magnets of lanthanides associating to other properties such as chirality, luminescence, and spin-crossover.



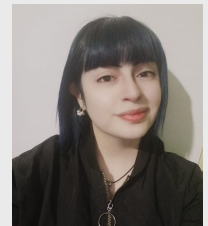
Patricio Hermosilla-Ibáñez is a researcher of the Centre for Development of Nanoscience and Nanotechnology (CEDENNA), Chile. His research focusses mainly on the crystallo-chemistry of coordination compounds of different dimensionality. Currently, he lead an project on the functionalization of carbon nanotubes with transition metal complexes for sensing applications.



Diego Venegas-Yazigi is a Full Professor of the Universidad de Santiago de Chile (USACH) and head of Molecular Magnetism and Molecular Materials Laboratory (LM⁴). Also, he is head of the Chemistry of Nanostructure group of CEDENNA. His research interest is related to the study of the structure and electronic properties of Polyoxometalates (POMs) and to the study of the magnetic properties of inorganic systems of different dimensionality.



Gabriela Paredes-Castillo is an undergraduate student of the Universidad de Santiago de Chile (USACH) and part of the Molecular Magnetism and Molecular Material Laboratory (LM⁴). Her research interest is related to the coordination chemistry of lanthanoid systems with magnetic and optical properties.



The thermal relaxation process in Ln^{III}-SIMs has been found to be dependent of three different relaxation mechanisms, Orbach^[17], Direct and Raman relaxation processes^[18–21]. The first is dominant at high temperatures and allows to obtain a value for the energy barrier of the relaxation of the magnetization (U_{eff}) and the relaxation time, τ_0 . In this sense, axiality favours higher U_{eff} values in Dy^{III} complexes, like in the $[\text{Dy}(\text{OtBu})_2(\text{py})_5]^+$ complex, which is formed by two negatively charged ligands along the principal axis, favouring axial coordination and weaker ligands in the equatorial plane, forming a pentagonal bipyramidal complex with D_{5h} symmetry. This system present one of the highest energy barriers reported in the literature of $U_{\text{eff}} = 1198 \text{ cm}^{-1}$ ^[22]. The Direct and Raman relaxation mechanisms occur through phonons, the Direct is a single-phonon process and the Raman is a two-phonon process, which has strong temperature dependence (T^n). Recently, several studies have reported n values different to 9 (Kramers ion`s) and 7 (non-Kramers ion`s), which is the original definition given by Orbach^[23], suggesting that values of $n \geq 4$, can be considered reasonable^[24–27]. Recent studies on the magnetic dynamic properties of these type of compounds have shown that phonon relaxation processes have an important contribution to the relaxation dynamics that need to be considered in order to describe properly the magnetic relaxation on Ln^{III}-SIMs^[28]. Finally, QTM is a thermally independent relaxation mechanism that causes deviations at low temperatures in the out-phase measurements^[29]. However, magnetic relaxation mechanism is still under studies since many features of the relaxation dynamics are not known. More detailed studies of magnetic Ln compounds are necessary to understand the dynamic of the relaxation process and the different mechanisms involved^[16,18,28,30–32] (Figure 1).

MINIREVIEW

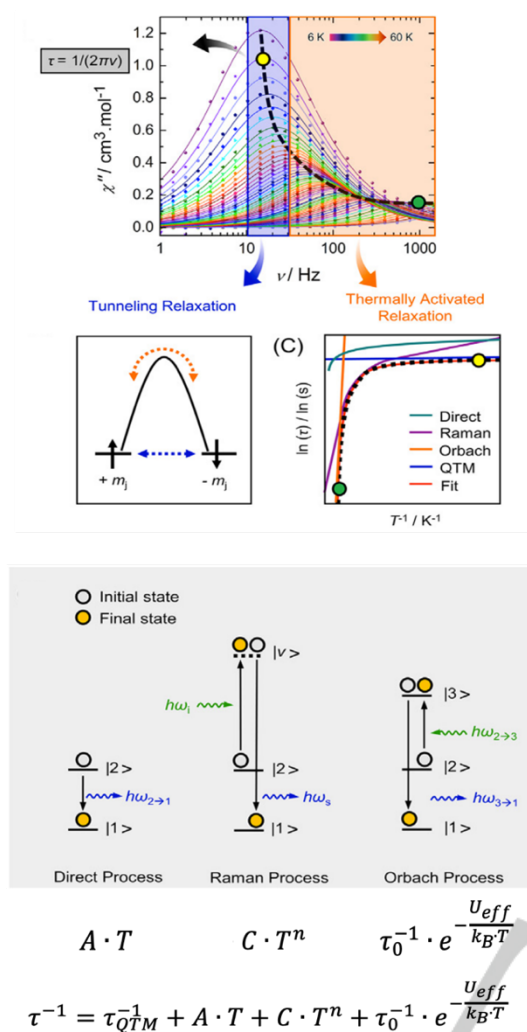


Figure 1. Relaxation dynamics mechanism observed in SIMs (Orbach, Direct, Raman and QTM). Adapted from ref. [29], Copyright (2019), with permission from Elsevier.

Most Ln-SIMs are based on organic ligands, in which the nature of these organic molecules together with the type and geometry of the Ln^{III} ion used (Kramer's or non-Kramer's ion), different features can be achieved, from large energy barriers to the modulation of relaxation mechanism (Ishikawa et al. [6] [NBu₄][TbPc₂] $U_{eff} = 584 \text{ cm}^{-1}$ and $\tau_0 = 6.25 \times 10^{-8} \text{ s}$; [NBu₄][DyPc₂] $U_{eff} = 28 \text{ cm}^{-1}$ and $\tau_0 = 6.25 \times 10^{-6} \text{ s}$). From the point of view of the Orbach thermal relaxation for homoleptic and heteroleptic organic Dy^{III} complexes, it is possible to observe that for octacoordinated systems, the U_{eff} values are in the same order of magnitude, as well as their relaxation times, τ_0 (Table 1) [6,33–35]. Nonetheless, a couple of cases present larger energy barriers up to 656 cm^{-1} , in which the coordination sphere of the Dy^{III} presents a N₄O₄ environment [36,37]. For these complexes the type, size, and disposition of the organic ligands, could be the causes of the large energy barriers observed. Moreover, it has been reported that heteroleptic complexes can favour SIM behaviour compared to homoleptic complexes [38]. However, both types of complexes (heteroleptic and homoleptic) present U_{eff} and τ_0 values all in the same order of magnitude for Dy^{III} complexes, thus, this is an assumption that still needs to be studied more in detail.

Table 1. X-Ray structure of organic based Dy^{III}-SIMs with the obtained energy barrier of magnetization (U_{eff}) and relaxation time (τ_0) are shown [6,33–35]. Where: acac = acetylacetonate, phen = 1,10-phenanthroline, Pc²⁻ = phthalocyaninate and 5,7-Cl₂q⁻ = 5,7-dichloro-8-hydroxyquinolate.

Formula	Structure	Relaxation
Dy(acac) ₃ (phen)]		$U_{eff} = 42 \text{ cm}^{-1}$ $\tau_0 = 5.7 \times 10^{-6} \text{ s}$
[DyPc ₂] ⁻		$U_{eff} = 28 \text{ cm}^{-1}$ $\tau_0 = 5.7 \times 10^{-6} \text{ s}$
[Dy(5,7-Cl ₂ q) ₄] ⁻		$U_{eff} = 60 \text{ cm}^{-1}$ $\tau_0 = 2.0 \times 10^{-6} \text{ s}$

Most of the SIMs synthesized are based on organic ligands while inorganic ligands have been relatively ignored, probably because the dimensionality of the final product is more complicated to control. Ln^{III}-SIMs based on inorganic ligands like Lacunary Polyoxometalates (LPOMs) are suitable to obtain systems with slow relaxation of the magnetization. The oxygen atoms localized in these lacunary zones are highly reactive forming a multidentate ligand, which makes possible to functionalize these structures with 4f metals ions, forming new coordination complexes [39–43]. Also, these LPOMs are diamagnetic and can provide an adequate magnetic insulation of the lanthanoid ion from the other neighbouring magnetic molecules in the crystal lattice [44]. These LPOMs are based on isopolyanions and heteropolyanions, in which the second ones are the most common inorganic ligands. In this ligands the heteroatom ($X^n = P^V, As^V, Si^IV, Ge^IV$) contribute to the stabilization of this species (Figure 2). Also, depending on the synthetic conditions this LPOMs can afford larger or smaller vacancies, which are related to the loss of tungstyl W=O units. However, most Ln^{III} complexes are based on the mono-lacunary Keggin species ($[XW_{11}O_{39}]^{n-}$) [45–47].

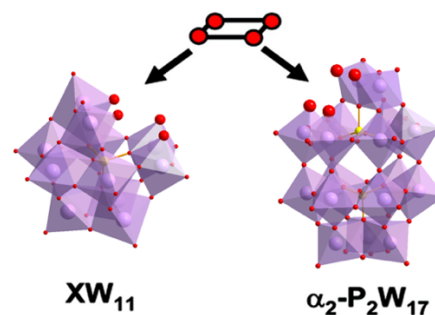


Figure 2. Lacunary species of the Keggin and Wells-Dawson structures, showing the vacancies. Light purple polyhedra correspond to MO₆.

MINIREVIEW

One of the first works on Ln-LPOMs SIMs was reported by AlDamen et al.^[7,47], in which, the Ln^{III} is encapsulated between two LPOMs, adopting in one case a square antiprismatic geometry for [Ln(W₅O₁₈)₂]⁹⁻ and in the second system a distorted square antiprism geometry is described for [Ln(SiW₁₁O₃₉)₂]¹³⁻. Unfortunately, only the X-ray structures of the Er^{III} and Tm^{III} compounds are reported. For the latter complexes, the only ones that present SIM behaviour are the Er^{III}, Dy^{III} and Yb^{III} analogues. Other fully inorganic (or homoleptic) Ln^{III} complexes have been reported in the literature with different heteroatoms (P^V and Ge^{IV}) observing different magnetic properties when the three systems are compared between each other.

Mononuclear hybrid (or heteroleptic) inorganic-organic Ln^{III} complexes with slow relaxation of the magnetization are difficult to reach. Most experimental attempts end with dinuclear systems like the ones with the Keggin mono-LPOMs, for example: [Ln(PW₁₁O₃₉)(bitartrate)]₂¹⁶⁻, [Ln(PW₁₁O₃₉)(H₂O)(acetate)]₂¹⁰⁻, [Ln(PW₁₁O₃₉)(H₂O)₂(oxalate)]¹⁰⁻, [Ln(PW₁₁O₃₉)(phen)(H₂O)]₂⁸⁻, among others^[48–51]. In these complexes the type and size of the organic ligand plays a crucial role since it is possible to obtain hepta- or octa-coordinated complexes. However, some examples of mononuclear system exist in the literature like, [Ln^{III}H(PW₁₁O₃₉)(phen)]₂⁴⁻, [Ln^{III}(PW₁₁O₃₉)(Pc)]⁶⁻, [Ln^{III}(GeW₁₁O₃₉)(H₂O)₄]⁵⁻ and [Ln^{III}(SiW₁₁O₃₉)(pdc)₂(H₂O)₂]⁹⁻^[46,52–54]. Finally, among all these systems, the Dy^{III}-based complexes with different types of organic ligands have been the most studied due to their magnetic properties.

Thus, in this review we present a study and comparison on the changes that inorganic and organic ligands can cause to the geometry of the metal centres of fully inorganic and hybrid (mononuclear and dinuclear) lanthanoid complexes (for Dy^{III}, Er^{III} and Yb^{III}). Moreover, we will discuss which of these changes can modify the magnetic properties of the Lanthanoid Complexes.

2. Synthesis of Inorganic and Hybrid Ln^{III} Complexes

Two different types of synthesis have been reported in the literature to obtain [Ln^{III}(LPOM)₂]ⁿ⁻, [Ln^{III}(LPOM)(L)_x]ⁿ⁻ and [Ln^{III}(LPOM)(L)_x]₂ⁿ⁻ systems: the traditional and solvothermal methods.

For the synthesis of mononuclear homoleptic inorganic complexes the traditional method is used. This synthetic method consist on the mixing of the Ln^{III} salts with the [XW₁₁O₃₉]ⁿ⁻ unit, where X = Si^{IV} or Ge^{IV}, at mild temperature conditions (50 – 80°C). A careful control of the pH (around 4.5 - 5) is done in order to avoid the transformation of the [XW₁₁O₃₉]ⁿ⁻ species into other LPOMs.^[55–57] On the other hand, for the synthesis of [Ln^{III}(PW₁₁O₃₉)₂]¹¹⁻, the literature reports that a different LPOMs is used as a precursor, such as, [P₂W₁₉O₆₉(H₂O)]¹⁴⁻ or [PW₉O₃₄]⁹⁻ species^[57,58].

For the synthesis of mononuclear heteroleptic Ln^{III} hybrid complexes the traditional and solvothermal synthesis have been reported. For the synthesis of [Dy^{III}(GeW₁₁O₃₉)(H₂O)₄]⁵⁻, the traditional synthetic approach is used, also with mild temperature conditions, and using [GeW₁₀O₃₆]⁸⁻ unit as precursor, maintaining the pH at 4.8^[46]. For the synthesis of [Ln^{III}(PW₁₁O₃₉)(phen)]₂⁴⁻ (**VUBLEM** (Dy^{III}) and **VUBLIQ** (Er^{III})) and [Ln^{III}(PW₁₁O₃₉)(Pc)]⁶⁻ (**GUZFOZ** (Tb^{III})), the same LPOM precursor is used, [NBu₄]₄[PW₁₁O₃₉H₃]^[59]. However, for the first complex solvothermal synthesis is used (T = 160°C for 2 days), with a

slightly variation of the pH at the beginning and the ending of the reaction time (pH_i = 5.0 and pH_f = 4.5)^[52]. For the second compound the synthesis considers a Ln^{III} compound precursor, [Ln^{III}(Ac)(Pc)], where Ac = CH₃COO⁻ and Pc²⁻ = phthalocyanine, which is mixed at room temperature in a mixture of solvents^[53].

Dinuclear complexes also can be obtained from traditional and solvothermal synthesis. For example, the acetate derivatives [Ln^{III}(XW₁₁O₃₉)(Ac)]₂ⁿ⁻ is synthesized by traditional methods maintaining the pH in range of 4.5 to 5, as described above, to avoid the transformation of the [XW₁₁O₃₉]ⁿ⁻ species and also under mild temperature conditions. The silicate and germanate LPOMs analogues (Dy^{III} = **ZIXCIV**, **DEGCID**, **ZOFKOW** and Er^{III} = **OGOSUF**, **ZOFKUC**, **ELIHEN**) are obtained using the same inorganic precursor, [XW₉O₃₄]¹⁰⁻ (X = Si^{IV} or Ge^{IV}) but the phosphate LPOM is synthesized with the mono-lacunary Keggin species, [PW₁₁O₃₉]⁷⁻^[49,60–62]. Another example of carboxylate derivatives are the dinuclear [Ln^{III}(XW₁₁O₃₉)(C₄H₂O₆)]₂¹⁶⁻ complexes (**WACJOC** (Dy^{III}), **WACJUI** (Er^{III}), **WACKP** (Yb^{III})), being synthesized with the inorganic [P₂W₁₉O₆₉(H₂O)]¹⁴⁻ precursor, under mild synthetic conditions (T = 60°C and ambient pressure)^[48]. Finally, it can be mentioned that most of the dinuclear compounds are based on carboxylate derivatives. However, a single case has been reported, in which a N-aromatic ligand is coordinating the dinuclear unit, forming the [Ln^{III}(PW₁₁O₃₉)(phen)(H₂O)]₂⁸⁻ complexes (**IFIPOF** (Pr^{III}), **IFIPUL** (Gd^{III}), **IFIQAS** (Sm^{III}), **IFIQEW** (La^{III}),) under hydrothermal synthesis. Interestingly, this is the only compound that is obtained not from a lacunary species but from the original Keggin POM^[63].

3. Structural Analysis

3.1. SHAPE Calculations

In order to describe the geometry distortions of the lanthanoid centres of the compounds the SHAPE code will be used to analyse the X-ray structures^[64]. This code permits to describe the geometry distortion by means of the continuous shape measurement (CShM's) of the Ln^{III} ions in the complex, by comparison of an ideal geometry with the experimental one. The determination of the correct X-ray structure is fundamental for the adequate evaluation of the magnetic properties.

Depending on the type of nature of the ligands that could be either fully inorganic or a hybrid system (inorganic-organic) the coordination number of these complexes are 7 and 8. For the 7 coordinated system 6 different types of geometry can be defined, while for the 8 coordinated systems, 13 different geometries can be obtained (Table 2)^[65,66]. However, it is possible to mention that most of the structures reported in the literature are octa-coordinated.

MINIREVIEW

Table 2. Coordination number (C.N.), Label, Shape and Symmetry group for hepta- and octa-coordinated geometries defined by the SHAPE code. In bold, most common geometries obtained.

C.N	Label	Shape	Symmetry
7	HP	Heptagon	D _{7h}
	HPY	Hexagonal pyramid	C _{6v}
	PBPY	Pentagonal bipyramid	D _{5h}
	COC	Capped octahedron	C_{3v}
	CTPR	Capped trigonal prism	C_{2v}
	JBPY	Johnson pentagonal bipyramid	D _{5h}
	JETPY	Elongated triangular pyramid	C _{3v}
8	OP	Octagon	D _{8h}
	HPY	Heptagonal pyramid	C _{7v}
	HBPY	Hexagonal bipyramid	D _{6h}
	CU	Cube	O _h
	SAPR	Square antiprism	D_{4d}
	TDD	Triangular dodecahedron	D _{2d}
	JGBF	Johnson - Gyrobifastigium	D _{2d}
	JETBPY	Johnson - Elongated triangular bipyramid	D _{3h}
	JBTP	Johnson - Biaugmented trigonal prism	C_{2v}
	BTPR	Bicapped trigonal prism	C_{2v}
	JSD	Snub disphenoid	D _{2d}
	TT	Triakis tetrahedron	T _d
	ETBPY	Elongated trigonal bipyramid	D _{3h}

3.2. Structural Databases Search

A complete search in the CCDC (Cambridge Crystallographic Data Centre) and ICSD (Inorganic Crystal Structure Database) of the lanthanoid (Ln^{III} = Dy^{III}, Er^{III} and Yb^{III}) complexes based on mononuclear (fully inorganic and hybrid) and dinuclear systems was done. Both CCDC and ICSD are defined in this work, as Crystallographic Structural Database (CSD). These results show that most of the systems are based on the mono-lacunary Keggin LPOM, [XW₁₁O₃₉]ⁿ⁻. Therefore, we have focussed our search on Ln^{III}-complexes with this LPOM. See the selected complexes in Table 3. CShM's calculations were done with SHAPE code to all the selected structures (See Tables S1, S2 and S3 in the Supporting Information).

3.3. Mononuclear Complexes

[Ln(XW₁₁O₃₉)₂]ⁿ⁻

These homoleptic complexes are "sandwich types" systems formed by two Keggin mono LPOMs that can be found with different heteroatoms (X), like P^V, Si^{IV} and Ge^{IV}. The four highly basic lacunary oxygens atoms of the Keggin LPOMs causes that the Ln^{III} ion adopt an octa-coordinated geometry, in particular a, SAPR geometry, which it is induce by the rigidity of the inorganic ligand.

Many examples of this types of complexes based on magnetic Ln^{III} ions can be found in the literature, such as: **KAMPUM** (Dy^{III}), **AWEQAW** (Er^{III}), **FARDOT** (Er^{III}), **1964368** (Dy^{III}), **1964360** (Er^{III}), **249433** (Yb^{III}) and **419267** (Er^{III}), according the CCDC and the ICSD^[47,55,58]. Complex **KAMPUM** correspond to K₂[N(CH₃)₄]₅H₄[Dy^{III}(PW₁₁O₃₉)₂]·28H₂O and it was reported by Ma et al.^[58]. In this case the electroneutrality is achieved by a combination of organic-inorganic cations, and four H⁺ that are delocalized over the crystal lattice. However, in the other cases the charge balance is achieved by only potassium cations (K⁺).

Interestingly, **1964368** (Dy^{III}) and **1964360** (Er^{III}) are part of family of compounds of formula [Ln^{III}(GeW₁₁O₃₉)₂]¹³⁻, in which it is observed that from the La^{III} to Dy^{III} the LPOMs corresponds to the α isomer, and from the Ho^{III} to Lu^{III} the inorganic ligands are formed by the [α-GeW₁₁O₃₉]⁸⁻ and [β-GeW₁₁O₃₉]⁸⁻^[55].

All the authors reported that the Ln^{III} ions adopt a SAPR geometry, as expected for complexes formed by rigid ligands with four coordination positions (lacunary oxygens). We have confirmed this by the SHAPE calculations of the CShM's parameters been the lowest of all 13 geometry possibilities with values ranging from 0.768 to 0.092 (Figure 3)

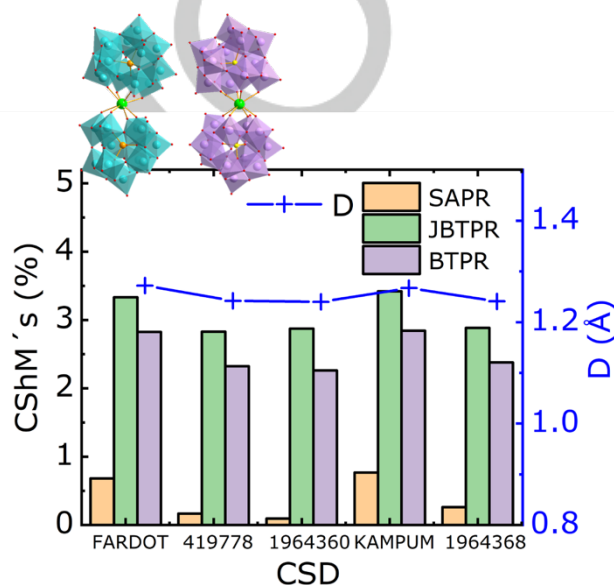


Figure 3. Lowest CShM's values of the SHAPE calculations for mononuclear inorganic Ln^{III} complexes, related to the D parameter. In light purple [PW₁₁O₃₉]⁷⁻ and in light blue [GeW₁₁O₃₉]⁸⁻.

Finally, it is possible to mention that this mononuclear Ln^{III}-LPOMs compounds can be found in the literature with Cu^I complexes as counter-cations or as connectors forming higher dimensionality systems. In particular, these complexes are form with the [AsW₁₁O₃₉]⁷⁻ and [SiW₁₁O₃₉]⁸⁻ fragments, being the former only found in the literature with Cu^I complexes, but not with other types of cations^[67].

[Ln(XW₁₁O₃₉)(L)_x]ⁿ⁻

A very interesting family of heteroleptic (or hybrid inorganic-organic) mononuclear complexes have recently reported in the literature, which are formed by a single LPOM unit. These compounds have a general formula [Ln^{III}(XW₁₁O₃₉)(L)_x]ⁿ⁻, where L correspond to the phen, H₂O or Pc²⁻ ligands, where their CCDC and ICSD codes are **VUBLEM** (Dy^{III}), **VUBLIQ** (Er^{III}), **ERTEO** (Yb^{III}), **1908052** (Dy^{III}) and **1908053** (Er^{III}).

VUBLEM and **VUBLIQ** were reported in 2019 by Cañón-Mancisidor et al.^[52] corresponding to the first mononuclear hybrid organic-inorganic Ln^{III} complex of formula [n-NBu₄]₃[Ln^{III}H(PW₁₁O₃₉)(phen)₂], in which a single H⁺ is delocalized all over the LPOM and being the geometry of the Ln^{III} ion defined as SAPR by the authors^[52]. Later the same authors reported in the literature the same family of complexes with different Ln^{III} ions, such as: Tb^{III}, Eu^{III}, Nd^{III}, Ho^{III} and Gd^{III}^[68]. On

MINIREVIEW

the other hand, a mononuclear complex based on the $[PW_{11}O_{39}]^{7-}$ and the organic ligand Pc^- was reported by Sarwar et al.^[53], being quite similar to the previously described systems. However, the authors did not report the X-ray structure of the Dy^{III} systems, only

informing the X-ray crystalline structure of the Y^{III} and Tb^{III} analogues. Thus, this system, will not be further discussed. Another hybrid system correspond to the complexes $K_5[Ln^{III}(GeW_{11}O_{39})(H_2O)_4]$ (**1908052** (Dy^{III}) and **1908053** (Er^{III}))^[46].

Table 3. Structural parameters of the mononuclear and dinuclear complexes based on the mono-lacunary Keggin LPOM, $[XW_{11}O_{39}]^{n-}$. The CSHM's values of the three lowest values, the D parameter in Å, and the type of ligand (inorganic and auxiliary) of the compound are presented. In colour the Ln^{III} complexes are highlighted, Dy^{III} (light green), Er^{III} (light purple) and Yb^{III} (light blue). In blue the lowest value of the SHAPE calculations is presented. The codes of the CSD are in letters for CCDC and in numbers for the ICSD.

Mononuclear									
C.N.	Complex	PBPY-7	COC-7	CTPR-7	JPBPY-7	D (Å)	CCDC / ICSD	Inorganic Ligand	Auxiliar Ligand
7	$[N(CH_3)_2]_{2.50}H_{2.50}[Yb(GeW_{11}O_{39})(H_2O)_2]$	6.877	1.854	0.492	10.139	0.840	RERTEO	$[GeW_{11}O_{39}]^{8-}$	H ₂ O
C.N.	Complex	SAPR-8	TDD-8	JBTPR-8	BTPR-8	D (Å)	CCDC / ICSD	Inorganic Ligand	Auxiliar Ligand
8	$K_5[Dy(H_2O)_4GeW_{11}O_{39}]$	1.236	2.734	1.816	0.760	0.839	1908052	$[GeW_{11}O_{39}]^{8-}$	H ₂ O
	$[n - NBu_4]_3(DyH(PW_{11}O_{39})(phen)_2)$	0.858	1.531	2.190	1.832	1.088	VUBLEM	$[PW_{11}O_{39}]^{7-}$	Phen
	$K_{13}[Dy(\beta_2 - GeW_{11}O_{39})_2]$	0.262	2.255	2.885	2.379	1.255	1964368	$[GeW_{11}O_{39}]^{8-}$	
	$K_2[N(CH_3)_4]_5H_4[Dy(\alpha - PW_{11}O_{39})_2]$	0.768	1.967	3.420	2.842	1.226	KAMPUM	$[PW_{11}O_{39}]^{7-}$	
	$K_{13}[Er(\beta_2 - SiW_{11}O_{39})_2]$	0.167	2.526	2.83	2.323	1.242	419267	$[SiW_{11}O_{39}]^{8-}$	
	$K_{13}[Er(PW_{11}O_{39})_2]$	0.682	2.078	3.332	2.827	1.272	FARDOT	$[PW_{11}O_{39}]^{7-}$	
	$K_{13}[Er(PW_{11}O_{39})_2]$	0.668	2.096	3.416	2.817	1.276	AWEQAW	$[GeW_{11}O_{39}]^{8-}$	
	$K_{13}[Er(\beta_2 - GeW_{11}O_{39})(\alpha - GeW_{11}O_{39})]$	0.092	2.512	2.872	2.26	1.240	1964360	$[GeW_{11}O_{39}]^{8-}$	
	$K_5[Er(H_2O)_4GeW_{11}O_{39}]$	1.619	3.131	1.311	1.320	0.723	1908053	$[GeW_{11}O_{39}]^{8-}$	H ₂ O
	$[n - NBu_4]_3(ErH(PW_{11}O_{39})(phen)_2)$	0.824	1.703	2.197	1.885	1.075	VUBLIQ	$[PW_{11}O_{39}]^{7-}$	Phen
	$K_{13}[Yb(\beta_2 - SiW_{11}O_{39})_2]$	0.174	2.45	2.836	2.343	1.258	249433	$[SiW_{11}O_{39}]^{8-}$	
Dinuclear									
C.N.	Complex	PBPY-7	COC-7	CTPR-7	JPBPY-7	D (Å)	CCDC / ICSD	Inorganic Ligand	Auxiliar Ligand
7	$[(CH_3)_4N]_{10}$ $\{[(\alpha - PW_{11}O_{39})_2Dy_2(H_2O)]_2(C_2O_4)\}$	5.737	0.799	1.223	9.416	0.933	DAQJOW	$[PW_{11}O_{39}]^{7-}$	H ₂ O - [C ₂ O ₄] ²⁻
	$[(CH_3)_4N]_{10}$ $\{[(\alpha - PW_{11}O_{39})_2Er_2(H_2O)]_2(C_2O_4)\}$	5.409	0.854	1.177	9.014	0.942	DAQKAJ	$[PW_{11}O_{39}]^{7-}$	H ₂ O - [C ₂ O ₄] ²⁻
	$(TBA)_{8.5}H_{1.5}$ $[(PW_{11}O_{39})_2Dy_2F_2(H_2O)_2]$	6.146	1.215	0.393	9.640	0.955	ZIXCER	$[PW_{11}O_{39}]^{7-}$	H ₂ O y F ⁻
	$(TBA)_{8.5}H_{1.5}$ $[(PW_{11}O_{39})_2Dy_2(OH)_2(H_2O)_2]$	6.159	1.433	0.446	9.113	0.822	ZIXCAN	$[PW_{11}O_{39}]^{7-}$	H ₂ O y OH ⁻
C.N.	Complex	SAPR-8	TDD-8	JBTPR-8	BTPR-8	D (Å)	CCDC / ICSD	Inorganic Ligand	Auxiliar Ligand
8	$(TBA)_{8.5}H_{1.5}$ $[(PW_{11}O_{39})_2Dy_2(CH_3COO)_2(H_2O)_2]$	2.695	2.516	1.656	0.989	0.989	ZIXCIV	$[PW_{11}O_{39}]^{7-}$	H ₂ O - Ac ⁻
	$Na_2[N(CH_3)_4]_4H_2$ $\{[Dy(\alpha - PW_{11}O_{39})(H_2O)_3]_2\}$	0.231	2.228	2.628	1.814	1.121	KAMQAT	$[PW_{11}O_{39}]^{7-}$	H ₂ O
	$[N(CH_3)_4]_6K_3H_7$ $[Dy(C_4H_2O_6)(\alpha - PW_{11}O_{39})_2]$	0.727	2.030	1.876	1.150	1.108	WACJOC	$[PW_{11}O_{39}]^{7-}$	[C ₄ H ₂ O ₆] ⁴⁻
	$[NH_2(CH_3)_2]_8$ $[Dy(H_2O)(pyCOO)(\alpha - HPW_{11}O_{39})_2]$	1.422	2.509	3.172	2.069	1.071	MERCOE	$[PW_{11}O_{39}]^{7-}$	[pyCOO] ⁻
	$[N(CH_3)_4]_{10}$ $\{[(\alpha - PW_{11}O_{39})_2Dy_2(H_2O)(CH_3COO)]_2\}$	1.499	2.246	2.807	1.926	1.142	DEGCID	$[PW_{11}O_{39}]^{7-}$	H ₂ O - Ac ⁻
	Na_4K_8 $\{[Dy(\alpha - SiW_{11}O_{39})(H_2O)]_2(\mu - CH_3COO)_2\}$	1.924	2.051	2.631	1.804	1.085	ZOFKOW	$[SiW_{11}O_{39}]^{8-}$	H ₂ O - Ac ⁻
	$[N(CH_3)_4]_{10}$ $\{[(\alpha - PW_{11}O_{39})_2Er_2(H_2O)(CH_3COO)]_2\}$	1.540	2.326	2.872	2.023	1.161	OGUSUF	$[PW_{11}O_{39}]^{7-}$	H ₂ O - Ac ⁻
	$[N(CH_3)_4]_6K_3H_7$ $[Er(C_4H_2O_6)(\alpha - PW_{11}O_{39})_2]$	0.613	2.048	1.962	1.211	1.089	WACJUI	$[PW_{11}O_{39}]^{7-}$	[C ₄ H ₂ O ₆] ⁴⁻
	Na_4K_8 $\{[Er(\alpha - SiW_{11}O_{39})(H_2O)]_2(\mu - CH_3COO)_2\}$	1.853	2.052	2.594	1.765	1.085	ZOFKUC	$[SiW_{11}O_{39}]^{8-}$	H ₂ O - Ac ⁻
	Na_4K_8 $\{[Er(CH_3COO)GeW_{11}O_{39}(H_2O)]_2\}$	1.83	2.233	2.558	1.662	1.050	ELIHEN	$[GeW_{11}O_{39}]^{8-}$	H ₂ O - Ac ⁻
	$[(CH_3)_2NH_2]_8$ $[Er(H_2O)(pyCOO)(\alpha - HPW_{11}O_{39})_2]$	1.111	2.768	3.12	2.091	1.057	EYOZUP	$[PW_{11}O_{39}]^{7-}$	[py-COO] ⁻ - H ₂ O
	$[(CH_3)_2NH_2]_8$ $[Er(H_2O)(pyCOO)(\alpha - HPW_{11}O_{39})_2]$	1.212	2.542	3.223	2.131	1.065	MERCIY	$[PW_{11}O_{39}]^{7-}$	[py-COO] ⁻ - H ₂ O
	$[N(CH_3)_4]_6K_3H_7$ $[Yb(C_4H_2O_6)(\alpha - PW_{11}O_{39})_2]$	0.612	2.115	1.728	1.206	1.092	WACKAP	$[PW_{11}O_{39}]^{7-}$	[C ₄ H ₂ O ₆] ⁴⁻
	Na_4K_8 $\{[Yb(CH_3COO)GeW_{11}O_{39}(H_2O)]_2\}$	1.737	2.429	2.321	1.399	0.985	ELIJIT	$[SiW_{11}O_{39}]^{8-}$	H ₂ O - Ac ⁻
	K_{13} $\{[Yb(\alpha - SiW_{11}O_{39})(H_2O)]_2(CH_3COO)_2\}$	1.842	2.251	2.35	1.564	1.040	ARICAF	$[GeW_{11}O_{39}]^{8-}$	H ₂ O - Ac ⁻

MINIREVIEW

The work describes the possibility that the metallic centre can be defined as nine-coordinated, however, this was discarded by the authors since one of the Dy-O(germanate) distance is over 2.8 Å, being too large to be considered as a coordination bond. Therefore, the geometry of the Ln^{III} ion was defined by the authors as SAPR. However, our SHAPE calculations show that the Ln^{III} ions are better described as a BTPR geometry.

Similar to this previously describe system, the **RETEO** complex is formed by the [Ln^{III}(GeW₁₁O₃₉)(H₂O)₂]⁵⁻, in which the Ln^{III} ion has a hepta-coordinated geometry and since the authors do not specify which one, our calculations show that the Yb^{III} centre adopts a CTPR geometry (CShM's value of 0.492). In this system an oxygen atom of a W=O fragment at a distance of 2.435(9) Å of a neighbour [GeW₁₁O₃₉]⁸⁻ coordinating the Ln^{III} ion to the closest [Ln^{III}(GeW₁₁O₃₉)(H₂O)₂]⁵⁻ unit forming a linear structure that propagates along the *b* axis.

Shape calculation of the Ln^{III} geometry for octa-coordinated complexes shows that the systems with the [PW₁₁O₃₉]⁷⁻ have larger CShM's parameter compared to their inorganic analogue, but still their geometry can be defined as SAPR (0.768 for **KAMPUM** and 0.858 **VUBLEM**). The higher distortion observed in the hybrid system can be attributed to the higher flexibility of the organic ligand (phen). However, for the systems formed by the [GeW₁₁O₃₉]⁸⁻ (**1908052** and **1908053**), the Ln^{III} geometry deviated more from the SAPR, as its geometry is better described as bicapped trigonal prism (BTPR or JBTPR) as mentioned above. This difference can be associated to a larger "bite angle" defined by Wang et al., which makes the lacunar site larger for Ge^{IV}, as discussed previously^[69]. Thus, the Ln^{III} ion may bind deeper into the lacunar site and together with the other ligands (in particular H₂O for this cases), causing that the metal ion adopts a bicapped trigonal geometry (Figure 4).

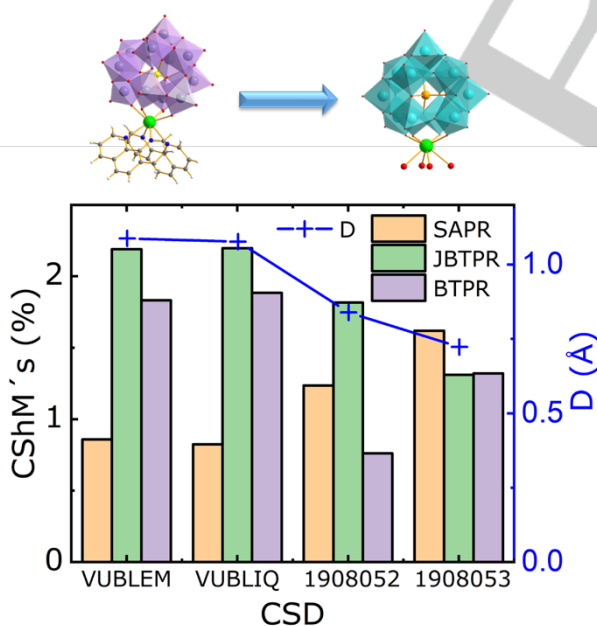


Figure 4. Lowest CShM's values of the SHAPE calculations for mononuclear hybrid Ln^{III} complexes, related to the D parameter. In light purple [PW₁₁O₃₉]⁷⁻ and in light blue [GeW₁₁O₃₉]⁸⁻.

To quantify this observation, we have defined the D parameter as the distance between the Ln^{III} ion and the best mean plane formed by the lacunary oxygens of the LPOM, so we can

measure how much the Ln^{III} ion can be displaced into the lacunar site (Figure 5). Thus, for the inorganic analogues [Ln^{III}(XW₁₁O₃₉)₂]ⁿ⁻ the D value is in the range of 1.226 to 1.276 Å, and all have a SAPR geometry. On the other hand, the **VUBLEM** which is a hybrid complex described also by a SAPR geometry has a D = 1.088 Å. However, for the **1908052** and **1908053** structures the D parameter are 0.839 and 0.723 Å, respectively. For both structures the Ln^{III} ion can be defined as bicapped trigonal prism. These results suggest that Ln^{III} ion adopting a SAPR geometry, present higher values of D.

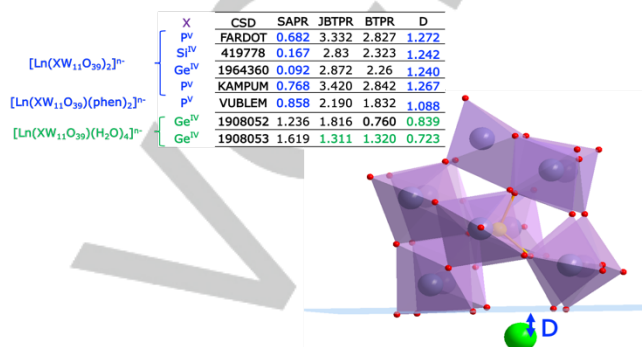


Figure 5. Displacement of the Ln^{III} ion into the best mean plane formed by the oxygen atoms of the lacunary site, D. Inset: Table showing the values of the D parameter and the lowest CShM's values associated to the most adequate geometry.

3.4. Dinuclear Complexes

Most of the hybrid inorganic-organic Ln^{III} complexes are dinuclear, and the metal centres can adopt seven and octa-coordinated geometries. The asymmetric unit of these complexes is mostly formed by a [Ln^{III}(XW₁₁O₃₉)(H₂O)]ⁿ⁻ unit with a bridging ligand, which together with the existence of an inversion centre, creates the dinuclear complex.

For systems with seven coordination number two families can be described, and all of them are formed by the [PW₁₁O₃₉]⁷⁻ unit. The first compound correspond to {[Ln^{III}(PW₁₁O₃₉)(ox)(H₂O)]₂}¹⁰⁻ reported by Zhang et al., where Ln^{III} = Dy^{III} (**DAQJOW**) and Er^{III} (**DAQKAJ**). A single oxalate molecule acts as bridging ligand connecting the two [Ln^{III}(PW₁₁O₃₉)(H₂O)]⁴⁻ units. According to the authors the metal centres adopts a CTPR geometry. However, our CShM's calculations shows that the Ln^{III} centres adopts a COC geometry. The correct description of the geometry of Ln^{III} complexes is important to study their magnetic properties. The second family of complexes is {[Dy^{III}(PW₁₁O₃₉)(L)(H₂O)]₂}¹⁰⁻, where L = F⁻ (**ZIXCER**) and OH⁻ (**ZIXCAN**), which acts as bridging ligands between [Ln^{III}(PW₁₁O₃₉)(H₂O)]⁴⁻ fragments. For both complexes, the Ln^{III} centres present a CTPR geometry as the CShM's values show^[70].

The other large family of hybrid (heteroleptic) dinuclear Ln^{III} complexes are mostly formed by organic ligands based on carboxylated molecules (RCOO⁻) except for the **KAMQAT** complex, which present H₂O molecules as auxiliary ligands, {[Dy^{III}(PW₁₁O₃₉)(H₂O)]₂}⁸⁻ with organic and inorganic counter-cations. In this complex the Ln^{III} ion presents a SAPR geometry as our SHAPE calculations show (CShM's value of 0.231). The dinuclear compound is formed by the coordination of an oxygen atom of the tungstyl unit of the [PW₁₁O₃₉]⁷⁻ fragment^[58].

The first complexes to be described are the ones formed by the tartaric unit as bridging ligand. These complexes have a

MINIREVIEW

general formula of $[(\text{CH}_3)_4\text{N}]_6\text{K}_3\text{H}_7\{[\text{Ln}^{\text{III}}(\text{PW}_{11}\text{O}_{39})(\text{C}_4\text{H}_2\text{O}_6)]_2\}$, where $\text{Ln}^{\text{III}} = \text{Dy}^{\text{III}}$ (**WACJOC**), Er^{III} (**WACJUI**) and Yb^{III} (**WACKAP**)^[48]. In these complexes, no water molecules exist as auxiliary ligands since the tartaric ligand presents various coordination groups (R-O^- and R-COO^-). The Ln^{III} ion present in all cases a SAPR geometry as shown by the SHAPE calculations, **WACJOC** (0.727), **WACJUI** (0.613) and **WACKAP** (0.612).

As mentioned above, most of these dinuclear complexes have a general formula of $\{[\text{Ln}^{\text{III}}(\text{XW}_{11}\text{O}_{39})(\text{H}_2\text{O})\text{L}]_2\}^{n-}$ where $\text{X} = \text{P}^{\text{V}}$, Si^{IV} and Ge^{IV} and $\text{L} = \text{pyCOO}^-$ and CH_3COO^- . These complexes are formed by the Keggin mono-LPMOs and the carboxylate derivatives acting as bridging ligands. The compounds with pyCOO^- ligands correspond to the **MERCOE** (Dy^{III}) and **EYOZUP/MERCIY** (Er^{III}). As final remark, of this three complexes, only the **EYOZUP** is reported in the literature by Li et al.^[71], the other two are only reported as CCDC Communications. The anionic complex corresponds to $\{[\text{Ln}^{\text{III}}(\text{PW}_{11}\text{O}_{39})(\text{H}_2\text{O})(\text{C}_5\text{NH}_4\text{COO})]_2\}^{10-}$ (where a H^+ is delocalized over the LPOM) and the electro-neutrality is achieved by the existence of 8 $[(\text{CH}_3)_2\text{NH}_2]^+$ molecules in the crystal lattice. In the three complexes the CShM's values suggest that the Ln^{III} ions have a SAPR geometry (Table 3). It is possible to comment that the large value obtained compared to other of the SAPR geometries discussed above could be related to the large size of the organic ligand that could induce a higher distortion of the first coordination sphere of the Ln^{III} centre.

To complete the structural description of these dinuclear compounds, the systems presenting the acetate molecule as bridging ligand with $\mu-1,1$ coordination mode are the ones more described in the literature. The complexes are formed by the anionic unit, $\{[\text{Ln}^{\text{III}}(\text{XW}_{11}\text{O}_{39})(\text{H}_2\text{O})(\text{CH}_3\text{COO})]_2\}^{10-}$, where $\text{X} = \text{P}^{\text{V}}$, Si^{IV} and Ge^{IV} , with organic or inorganic cations in the crystal lattice to achieve electroneutrality. The complexes found in the literature for Dy^{III} are **ZIXCIV** (P^{V}), **DEGCID** (P^{V}) and **ZOFKOW** (Si^{IV}); for Er^{III} **OGUSUF** (P^{V}), **ZOFKUC** (Si^{IV}) and **ELIHEN** (Ge^{IV}); and for Yb^{III} **ARICAF** (Si^{IV}) and **ELIJIT** (Ge^{IV}). All the Ln^{III} centres are octa-coordinated, in which the SHAPE calculation reflects that lower values of CShM's are related to the SAPR, BTPR and TDD geometries (Table 3). These results also show an interesting feature as a general tendency, in which the LPOM formed by P^{V} tends to adopt a SAPR geometry, in contrast with the ones formed by the tetravalent heteroatoms (Si^{IV} and Ge^{IV}) that tends to adopt a bicapped trigonal prism geometries (BTPR and JBTPR).

These results can be analysed by comparing the CShM's values of the Er^{III} compounds since it present the same inorganic ligand, $[\text{XW}_{11}\text{O}_{39}]^{n-}$ with $\text{X} = \text{P}^{\text{V}}$, Si^{IV} and Ge^{IV} and also the same organic ligands (CH_3COO^-). For **OGUSUF**, the lowest CShM's value is 1.540 for the SAPR geometry. However, for the **ZOFKUC** and **ELIHEN** compounds the CShM's values for the SAPR (1.853 and 1.830) are larger than to the ones of the BTPR geometry (1.765 and 1.662). These results can rationalize using the D parameter previously described for mononuclear systems, being the D values for **OGUSUF** (1.161 Å), **ZOFKUC** (1.085 Å) and **ELIHEN** (1.050 Å). For the Dy^{III} and Yb^{III} complexes a similar trend is observed. These results show that the change in the heteroatoms affects the size of the lacunar site, meaning that indirectly the nature of the heteroatom induces changes in the Ln^{III} geometry (Figure 6).

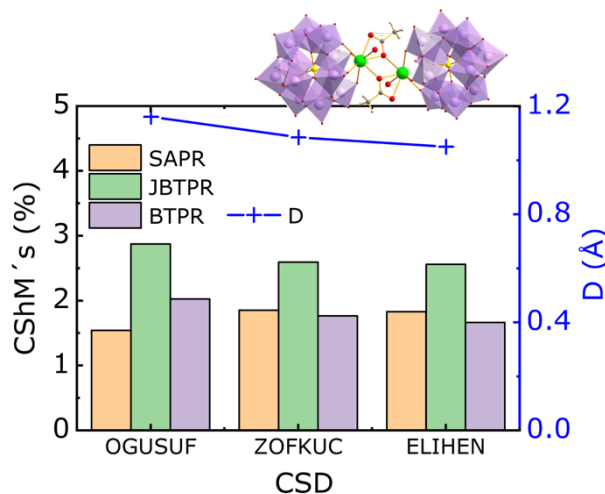


Figure 6. Lowest CShM's values of the SHAPE calculations for dinuclear acetate hybrid Er^{III} complexes, related to the D parameter. All complexes have the same structure except for the heteroatom of the LPOMs: **OGUSUF** (P^{V}), **ZOFKUC** (Si^{IV}) and **ELIHEN** (Ge^{IV}).

4. Magnetic Properties

4.1. Static (dc) Magnetic Properties

The static (*dc*) magnetic properties of the mononuclear inorganic Ln^{III} complexes are in good agreement with those expected for an isolated Dy^{III} ($S = 5/2$, $L = 5$, ${}^6\text{H}_{15/2}$, $g = 4/3$, $\chi T = 14.17 \text{ emu K mol}^{-1}$), Er^{III} ($S = 3/2$, $L = 6$, ${}^4\text{I}_{15/2}$, $g = 36/5$, $\chi T = 11.48 \text{ emu K mol}^{-1}$) and Yb^{III} ($S = 1/2$, $L = 3$, ${}^2\text{F}_{7/2}$, $g = 8/7$, $\chi T = 2.57 \text{ emu K mol}^{-1}$) centres. For example for the $[\text{Dy}^{\text{III}}(\text{PW}_{11}\text{O}_{39})_2]^{11-}$ (**KAMPUM**) the χT value at room temperature is $14.5 \text{ emu K mol}^{-1}$, for $[\text{Dy}^{\text{III}}(\text{SiW}_{11}\text{O}_{39})_2]^{13-}$ (**No X-ray data**) is $13.7 \text{ emu K mol}^{-1}$ and for $[\text{Dy}^{\text{III}}(\text{GeW}_{11}\text{O}_{39})_2]^{13-}$ (**1964368**) is $13.6 \text{ emu K mol}^{-1}$. This is related to the large size of the LPOM and to the diamagnetic nature of the inorganic ligand, providing an adequate magnetic insulation of the lanthanoid ion from the other neighbouring magnetic molecules in the crystal lattice. Therefore, the decrease in the χT values is due to the thermal depopulation of the energy levels of the respective split ground terms. For the hybrid inorganic-organic (heteroleptic) Ln^{III} complexes a similar trend is observed, since for $[\text{Dy}^{\text{III}}(\text{PW}_{11}\text{O}_{39})(\text{phen})_2]^{4+}$ (**VUBLEM**) the χT value at room temperature is $14.1 \text{ emu K mol}^{-1}$ and for $[\text{Dy}^{\text{III}}(\text{PW}_{11}\text{O}_{39})(\text{Pc})]^{6-}$ (**No X-ray data**) the value is $13.26 \text{ emu K mol}^{-1}$.

For the dinuclear hybrid Ln^{III} complexes most of the magnetic *dc* studies are related to system with carboxylate derivatives, with a few examples with H_2O , OH^- or F^- , as bridging ligands, and also with different geometries. For the first types of Dy^{III} complexes, like **ZIXCIV** (acetate) and **WACJOC** (tartrate), which are octa-coordinated, the susceptibility (per centre) at room temperature are in good agreement with those expected for an isolated Dy^{III} , suggesting that no exchange interaction exists between lanthanoid ions. For, hepta-coordinated complexes with the F^- (**ZIXCER**) and OH^- (**ZIXCAN**), as bridging ligands, present a χT value per centre at room temperature of c.a. $13.9 \text{ emu K mol}^{-1}$. The size of the bridging ligands could indicate that the metal centres are closer inducing some type of magnetic interaction between the Dy^{III} ions. Moreover, **ZIXCER** presents an increase

MINIREVIEW

of the susceptibility values at low temperature, suggesting the presence of ferromagnetic interactions between the Dy^{III} centres, which has been reported previously for fluoride-bridged lanthanide compounds^[72].

4.1. Dynamic (ac) Magnetic Properties

For the mononuclear inorganic systems, the *ac* susceptibility data of the Er^{III} and Dy^{III} analogues have been reported, being some examples, [Er(SiW₁₁O₃₉)₂]¹³⁻ (**419267**), [Dy(SiW₁₁O₃₉)₂]¹³⁻ (**No X-ray data**), [Dy(PW₁₁O₃₉)₂]¹¹⁻ (**KAMPUM**), [Er(GeW₁₁O₃₉)₂]¹³⁻ (**1964360**) and [Dy(GeW₁₁O₃₉)₂]¹³⁻ (**1964368**) with no report of the *ac* magnetic data for [Yb(XW₁₁O₃₉)₂]ⁿ⁻ complexes. Due to the rigidity of the inorganic ligands all these complexes have SAPR geometry. For all this complexes, not all the crystal structures are reported and even more, the analysis of the dynamic properties has not been extensively done.

For the complexes with the Si^{IV} as heteroatom, [Er(SiW₁₁O₃₉)₂]¹³⁻ (**419267**) and [Dy(SiW₁₁O₃₉)₂]¹³⁻ (**No X-ray data**), both systems present frequency dependent signals under a zero *dc* field, but no maxima, suggesting that QTM mechanism is dominant, but no study was reported under an applied *dc* field^[47]. However, we still can do some analysis of the dynamic properties with the available data. The Er^{III} system presented in this work [Er(SiW₁₁O₃₉)₂]¹³⁻ have SIM behaviour under zero *dc* field, but no maxima are observed. In contrast, Mougharbel et al.^[55] reported [Ln^{III}(GeW₁₁O₃₉)₂]¹³⁻ complexes, in which the Er^{III} analogue present SIMs behaviour under an applied *dc* field of 500G (U_{eff} = 43 cm⁻¹ and τ₀ = 6.0 × 10⁻⁹ s). These results suggest that the complex with the [SiW₁₁O₃₉]⁸⁻ ligands could present maxima if a *dc* field is applied in the study.

For the case of inorganic Dy^{III}-SIMs, the [Dy(PW₁₁O₃₉)₂]¹¹⁻ system do not present a dynamic response under zero *dc* field, but at 3 kG, a dynamic response is observed, allowing to obtained the energy barrier of magnetization and relaxation time (U_{eff} = 36.3 cm⁻¹ and τ₀ = 9.6 × 10⁻¹² s)^[58]. For the [Dy(SiW₁₁O₃₉)₂]¹³⁻ complex that has the same molecular anionic species, being the only difference the heteroatom (P^V → Si^{IV}), the system present SIM behaviour at zero field with a strong frequency dependent signals but no maxima are observed, a clear difference with the [Dy^{III}(PW₁₁O₃₉)₂]¹¹⁻ complex. Moreover, a [Dy^{III}(GeW₁₁O₃₉)₂]¹³⁻ complex do not presented SIM properties as described by Mougharbel et al.^[55]. Thus, for the case of the Dy^{III} complexes the nature of the heteroatom in the LPOM seems to have an influence in the SIM behaviour due to the larger vacancy observed for the Ge^{IV} systems that causes a change in the Dy^{III} geometry (Table 4).

For mononuclear heteroleptic (LPOM + auxiliary ligand) Ln^{III}-SIMs only a few examples exist in the literature, [Dy^{III}(PW₁₁O₃₉)(phen)₂]⁴⁻ (**VUBLEM**), [Er^{III}(PW₁₁O₃₉)(phen)₂]⁴⁻ (**VUBLIQ**), [Dy^{III}(PW₁₁O₃₉)(Pc)]⁶⁻ (**No X-ray data**) and [Dy^{III}(GeW₁₁O₃₉)(H₂O)₄]⁵⁻ (**1908052**)^[3,52,53]. The dynamic properties of the first Dy^{III} compound were studied under an applied *dc* field of 2000 kG, with the best fit parameters of U_{eff} = 36.4 cm⁻¹, τ₀ = 5.3 × 10⁻⁹ s, τ_{QTM} = 0.021 s, A = 8.61 s⁻¹ K⁻¹, n = 3.65 and C = 0.997 K⁻ⁿ s⁻¹ (Figure 7)^[52]. The Ln^{III} ion have SAPR geometry like its inorganic analogue [Dy^{III}(PW₁₁O₃₉)₂]¹¹⁻. The [Dy^{III}(PW₁₁O₃₉)(phen)₂]⁴⁻ is a SIM with U_{eff} = 36.4 cm⁻¹ considering the Orbach relaxation mechanism under an optimal field of 2 kG (the optimum field corresponds to the magnetic field that shifts the

relaxation to the slowest frequency). The hybrid complex is more efficient than its purely inorganic analogue. First, the optimum field is lower (2 kG vs. 3 kG); second, the relaxation time (τ₀) is slowed down by 3 orders of magnitude (5.3 × 10⁻⁹ s vs 9.6 × 10⁻¹² s); third, U_{eff} is unaffected around 36 cm⁻¹. Moreover, Sarwar et al.^[53] reported the dynamic properties of a second hybrid Ln^{III}-SIMs, [Dy^{III}(PW₁₁O₃₉)(Pc)]⁶⁻, however, no X-ray structure was reported. The best fit parameters were obtained under an applied *dc* field of 0.5 kG, with U_{eff} = 33.7 cm⁻¹, τ₀ = 1.1 × 10⁻⁷ s, A = 8.9 s⁻¹ K⁻¹, n = 4.9 and C = 0.41 K⁻ⁿ s⁻¹ (Table 4) The values reported for the thermal relaxation are similar to the ones obtained for [Dy^{III}(PW₁₁O₃₉)(phen)₂]⁴⁻, with the exception that lower *dc* field is needed. Thus, the addition of organic ligands seems to improve the magnetization dynamics in Dy^{III}-POM compounds. This could be due to the fact that the [Dy^{III}(PW₁₁O₃₉)(phen)₂]⁴⁻ complex is an heteroleptic system that can favours SIM behaviour compared to the inorganic analogue, which is an homoleptic system. Moreover, the behaviour could also be influenced by the nature the organic ligands, which are anionic or neutral with oxygen or nitrogen atoms coordinating the Dy^{III} centre altering the effective charge distribution over the metal ion. Also, the type of ligand, aliphatic or aromatic, may have an effect on the dynamic magnetic properties since they can induce distortions on the coordination geometry. Therefore, the above could induce subtle modifications on Ligand Field affecting the relaxation dynamics, which are sensitive to these variables^[14,73].

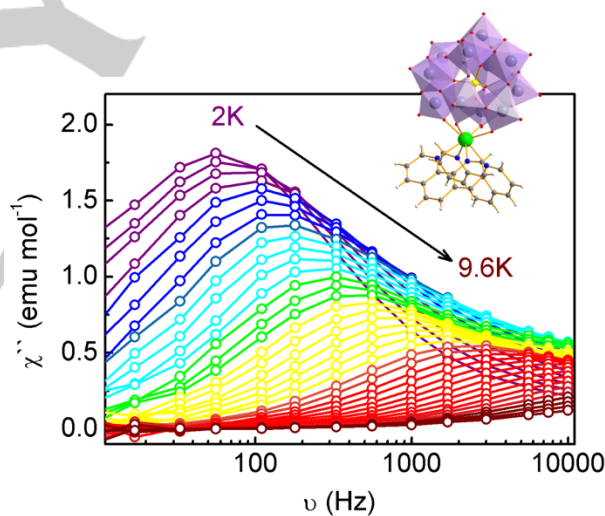
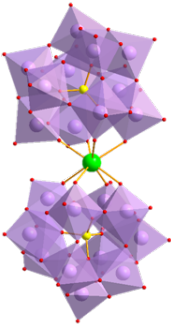
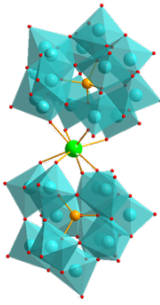
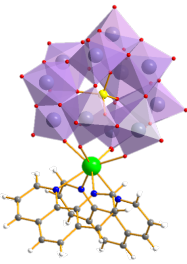
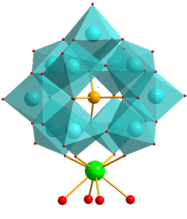


Figure 7. X-ray structure of [Dy^{III}(PW₁₁O₃₉)(phen)₂]⁴⁻ and out-of-phase (χ'') components of the *ac* magnetic susceptibility in 2 kOe external *dc* field. Adapted from ref.^[52], Copyright (2019), with permission from Royal Society of Chemistry.

As was mentioned above, when describing the relaxation dynamics of Dy^{III} and Er^{III} complexes with [XW₁₁O₃₉]ⁿ⁻ ligands, where X = Ge^{IV}, Si^{IV} and P^V, it is possible to infer that for the inorganic Dy^{III} compounds, [Dy^{III}(PW₁₁O₃₉)₂]¹¹⁻ and [Dy^{III}(SiW₁₁O₃₉)₂]¹³⁻ both presented different dynamic properties. If then we compare the dynamic magnetic properties of both systems with the [Dy^{III}PW₁₁O₃₉)₂(phen)₂]⁴⁻ complex, it is possible to observed that the hybrid system has a similar dynamic response compared to the [Dy^{III}(SiW₁₁O₃₉)₂]¹³⁻. Both present strong frequency dependent signals but no maxima, while the [Dy^{III}(PW₁₁O₃₉)₂]¹¹⁻ do not have any signal at zero *dc* field. In the case of the [Er^{III}(PW₁₁O₃₉)₂(phen)₂]⁴⁻ complex, the system present

MINIREVIEW

Table 4. X-Ray structures of inorganic and hybrid mononuclear based Dy^{III}-SIMs with their relaxation dynamics studies obtained by the authors. The Orbach, Raman, Direct and QTM processes are shown.

Complex	[Dy(PW ₁₁ O ₃₉) ₂] ¹¹⁻	[Dy(SiW ₁₁ O ₃₉) ₂] ¹¹⁻	[Dy(GeW ₁₁ O ₃₉) ₂] ¹¹⁻
CCDC/ICSD	KAMPUM	No X-ray data	1964368
Structure		* The authors report the complex, but they do not inform the X-ray structure.	
H _{dc} (kG)	4	* The authors report that the system present frequency dependent signals at zero dc field, but no study under an applied dc field is done. So, no analysis of the relaxation dynamics is done.	* The authors report that the system does not present frequency dependent signals at zero dc field. No further analysis is done.
U _{eff} (cm ⁻¹)	36.3		
τ ₀ (s)	9.6 × 10 ⁻¹²		
n	Not evaluated		
C (s ⁻¹ K ⁻ⁿ)	Not evaluated		
A (s ⁻¹ K ⁻¹)	Not evaluated		
τ _{QTM} (s)	Not evaluated		
Complex	[Dy ^{III} (PW ₁₁ O ₃₉)(phen) ₂] ⁴⁻	[Dy ^{III} (GeW ₁₁ O ₃₉)(H ₂ O) ₄] ⁵⁻	[Dy ^{III} (PW ₁₁ O ₃₉)(Pc)] ⁶⁻
CCDC/ICSD	VUBLEM	1908052	No X-ray data
Structure			* The authors report the complex, but they do not inform the X-ray structure.
H _{dc} (kG)	2	* The authors report that the system present frequency dependent signals at zero dc field. The authors perform field dependency studies, but they weren't able to study the relaxation dynamics	0.5
U _{eff} (cm ⁻¹)	36.4		33.7
τ ₀ (s)	5.3 × 10 ⁻⁹		1.1 × 10 ⁻⁷
n	3.65		4.9
C (s ⁻¹ K ⁻ⁿ)	0.997		0.41
A (s ⁻¹ K ⁻¹)	8.61		8.9
τ _{QTM} (s)	0.021		Not evaluated

SIM behaviour, but the QTM is dominant even at high fields, and when we compare the Orbach relaxation mechanism of this system with other inorganic analogues, [Er^{III}(SiW₁₁O₃₉)₂]¹³⁻ and [Er(GeW₁₁O₃₉)₂]¹³⁻, it is possible to observed that both complexes show SIMs properties, however, only for the second one the U_{eff} and τ₀ values are reported under an applied dc field.

Mononuclear hybrid inorganic-organic Ln^{III} complexes with slow relaxation of the magnetization are difficult to reach. As mentioned above, most experimental attempts end with dinuclear systems with the Keggin mono-LPOM with a carboxylate type

ligand that have a μ_{1,2}- and μ_{1,1}-coordination mode and the coordination sphere is completed with a H₂O molecule presenting an octa-coordinated environment, with a SAPR geometry for the Ln^{III} ion. Of the different types of carboxylate ligands only the one with bitartrate present a study of the relaxation dynamic for the Dy^{III} compound, {[Dy^{III}(PW₁₁O₃₉)(bitartrate)]₂}¹⁶⁻ (**WACJOC**)^[48]. For this compound, frequency dependent signals are observed under a zero dc field but with no maxima (QTM is dominant under this condition). Only with high dc field of 4 kG, clear maxima are observed. The relaxation dynamics was only study considering

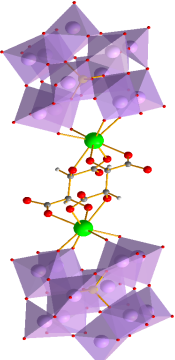
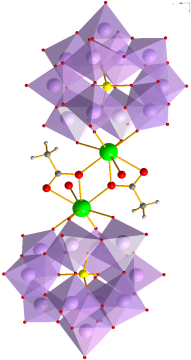
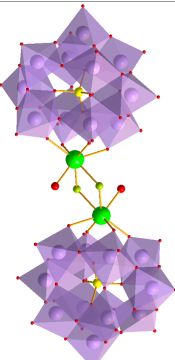
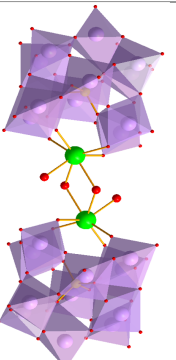
MINIREVIEW

the Orbach mechanism, with the best fit parameters of $U_{\text{eff}} = 13 \text{ cm}^{-1}$ and $\tau_0 = 4.2 \times 10^{-7} \text{ s}$ (Table 5). However, it is clear by the temperature dependence of the relaxation time that other mechanisms exist, like the Direct (AT) and/or Raman (CT^n) ones.

Other example in which the dynamic properties of a dinuclear systems are presented is the work of Huo et al.^[70], in

which the effect of bridging ligands on magnetic behaviour in dinuclear dysprosium systems are studied. Three different complexes are reported, $\{[\text{Dy}^{\text{III}}(\text{XW}_{11}\text{O}_{39})(\text{H}_2\text{O})(\text{CH}_3\text{COO})]_2\}^{10-}$ (**ZIXCIV**), $\{[\text{Dy}^{\text{III}}(\text{PW}_{11}\text{O}_{39})(\text{F})(\text{H}_2\text{O})]_2\}^{10-}$ (**ZIXCER**) and $\{[\text{Dy}^{\text{III}}(\text{PW}_{11}\text{O}_{39})(\text{OH})(\text{H}_2\text{O})]_2\}^{10-}$ (**ZIXCAN**). In the first system the Dy^{III} centre presents a SAPR geometry, and no analysis of the

Table 5. X-Ray structures of hybrid dinuclear based Dy^{III} -SIMs with the relaxation dynamics studies done by the authors. The Orbach, Raman, Direct and QTM processes are shown.

Complex	$\{[\text{Dy}^{\text{III}}(\text{PW}_{11}\text{O}_{39})(\text{bitartrate})]_2\}^{16-}$	$\{[\text{Dy}^{\text{III}}(\text{PW}_{11}\text{O}_{39})(\text{H}_2\text{O})(\text{CH}_3\text{COO})]_2\}^{10-}$
CCDC/ICSD	WACJOC	ZIXCIV
Structure		
H_{dc} (kG)	4	* The authors report that the system present frequency dependent signals at zero dc field. At 1000 G, the system present frequency dependent signals but no maxima are observed. No analysis of the relaxation dynamics is done.
U_{eff} (cm^{-1})	13	
τ_0 (s)	4.2×10^{-7}	
n	Not evaluated	
C ($\text{s}^{-1} \text{K}^{-n}$)	Not evaluated	
A ($\text{s}^{-1} \text{K}^{-1}$)	Not evaluated	
τ_{QTM} (s)	Not evaluated	
Complex	$\{[\text{Dy}^{\text{III}}(\text{PW}_{11}\text{O}_{39})(\text{F})(\text{H}_2\text{O})]_2\}^{10-}$	$\{[\text{Dy}^{\text{III}}(\text{PW}_{11}\text{O}_{39})(\text{OH})(\text{H}_2\text{O})]_2\}^{10-}$
CCDC/ICSD	ZIXCER	ZIXCAN
Structure		
H_{dc} (kG)	0	0
U_{eff} (cm^{-1})	74	98
τ_0 (s)	1.55×10^{-8}	8.74×10^{-9}
n	1.02	1.60
C ($\text{s}^{-1} \text{K}^{-n}$)	117	3.2
A ($\text{s}^{-1} \text{K}^{-1}$)	Not evaluated	Not evaluated
τ_{QTM} (s)	Not evaluated	Not evaluated

MINIREVIEW

dynamic response is done, because according to the authors the system does not present SMM behaviour, since no maxima appear in the *ac* susceptibility measurements under zero *dc* field. However, under a *dc* field of 1 kG, frequency dependent signals appear, suggesting that the compound is a field induce systems.

The two other complexes are hepta-coordinated systems, presenting in both cases CTPR geometry for the Dy^{III} centres. The coordination sphere is formed by one [PW₁₁O₃₉]⁷⁻, one H₂O and two OH⁻ (or F⁻) ions, which acts as bridging ligands. These system presents frequency dependent signals, under zero *dc* field, being the susceptibility data successfully fitted considering two relaxation processes, but the relaxation times obtained are meaningless since the maxima are too broad and too fast. For both complexes, the relaxation dynamics was studied in the high temperature range considering the Orbach mechanism, with $U_{\text{eff}} = 75 \text{ cm}^{-1}$, $\tau_0 = 1.05 \times 10^{-8} \text{ s}$. for **ZIXCER** and $U_{\text{eff}} = 101 \text{ cm}^{-1}$, $\tau_0 = 6.39 \times 10^{-9} \text{ s}$ for **ZIXCAN**. Moreover, the authors were able to study the complete relaxation dynamics (all temperature range) by considering the Raman + Orbach processes. The best fit parameters obtained are $U_{\text{eff}} = 74 \text{ cm}^{-1}$, $\tau_0 = 1.55 \times 10^{-8} \text{ s}$, $n = 1.02$ and $C = 117 \text{ K}^{-n} \text{ s}^{-1}$ for **ZIXCER** and $U_{\text{eff}} = 98 \text{ cm}^{-1}$, $\tau_0 = 8.74 \times 10^{-9} \text{ s}$, $n = 1.60$ and $C = 3.2 \text{ K}^{-n} \text{ s}^{-1}$ for **ZIXCAN** (Table 5). These results present different features, like the Orbach relaxation process is correctly describe since both fits give similar results, and that the energy barrier of magnetization is relatively high among POM based Ln^{III} systems. This could be related to the distances of the coordinating atoms of the ligands (LPOM and organic). In the case of **ZIXCAN**, the average distances are 2.259 Å and 2.434 Å, for the Dy^{III}-O(LPOM) and Dy^{III}-O(H₂O - OH⁻) bonds, respectively. While **VUBLEM** shows an average distance of 2.298 Å for the Dy^{III}-O(LPOM) bonds and 2.576 Å for the Dy^{III}-N(phen) bonds. For **ZIXCIV**, the average distances are 2.295 Å and 2.467 Å, for the Dy^{III}-O(LPOM) and Dy^{III}-O(H₂O - Ac⁻) bonds, respectively. This data could suggest that when the coordinating atoms are closer to the Dy^{III} ion, the U_{eff} value increases, as suggested by Costes et al.^[74]. Thus, this observation may explain the large U_{eff} value observed for **ZIXCAN** and why the other two systems mentioned have a smaller dynamic magnetic response. However, this statement must be treated with caution since the geometry and magnitude of the axiality of the Ligand Field around the metal centres are different, being **ZIXCAN** hepta-coordinated system and **VUBLEM** and **ZIXCIV** are octa-coordinated. For the Raman type magnetic relaxation, the low value of the *n* parameter observed for [Dy^{III}(PW₁₁O₃₉)(phen)₂]⁴⁻ (**VUBLEM**) and [Dy^{III}(PW₁₁O₃₉)(Pc)]⁶⁻ (**No X-ray data**) indicates that both acoustic (lattice) and optical (molecular) vibrations are involved in the process^[24]. Finally, it is possible to postulate that the relaxation dynamics in this type of coordination compounds, would be influence by the changes in the nature of the heteroatom of the LPOMs. Since, the Ln^{III} centre could penetrate more in the lacunary vacancy, inducing changes in the geometry of the metal ion that also should shorten the Ln^{III}-O(LPOM) bond distances. These changes in the geometry, together with the type and nature of the organic ligands, which can affect the effective charge distribution around the Ln^{III} ion, could in consequently, modify their crystal field parameters and therefore, will influenced the dynamic magnetic properties. Nonetheless, more studies are necessary to understand the magnetic properties of these systems and remains as an open subject.

5. Conclusions and Outlook

The X-ray structural data reveals by means of the Continuous Shape Measurements (CSHM's) and the D parameter that changing the nature of the heteroatom of the LPOMs change the geometry of the Ln^{III} ion, from SAPR to BTPR. Thus, these structural changes can be related in modifications in the magnetic properties of this type of system.

In general, these studies have estimated U_{eff} values between 13 to 36 cm⁻¹, for octa-coordinated systems, either mononuclear or dinuclear complexes. The highest U_{eff} value is 36 cm⁻¹ and an intrinsic relaxation time (τ_0) between 10⁻⁷ to 10⁻¹² s, being all these values obtained under an applied *dc* field. This could be related to the existence of QTM, but the field dependency studies have been not enough to properly study the relaxation dynamics of this complexes. For all the octa-coordinated complexes, quantum tunnelling exists, only in some cases it can be quenched by applying a *dc* field as high as 4 kG.

Mononuclear hybrid Ln^{III}-SIMs gives birth to a new family of molecules with slow relaxation of the magnetization that can be tuned by changing the nature and type of the organic and/or the inorganic ligand. No Yb^{III} hybrid complex with SIMs properties have been reported.

For dinuclear systems, seven coordinated system are presented, being the one that gives the higher U_{eff} value for a Ln^{III}-LPOM complex, 98 cm⁻¹. For the octa-coordinated systems, the U_{eff} values are smaller or are not informed.

Finally, it is possible to mention that most studies have been reported using the Orbach process, which do not permit a comprehensive study of the relaxation dynamics. The phonon-like relaxation (Raman + Direct) together with the temperature independent phenomena (τ_{QTM}) have been informed in a reduced number of studies (3 for Dy^{III}).

6. Acknowledgements

WCM thanks FONDECYT Regular 1211282 and ECOS 200027 (C20E04) for financial support. DVY thanks FONDECYT Regular 1201249. The author's thank research project Financiamiento Basal Program AFB180001. The authors thanks FONDEQUIP-EQM130086. This work was done under the LIA-M3-1027 CNRS Collaborative Program. We thank Guillermo Mínguez Espallargas for fruitful discussions.

Keywords: Lanthanoid • Lacunary Polyoxometalates • Keggin • Single Ion Magnets • Magnetic Relaxation

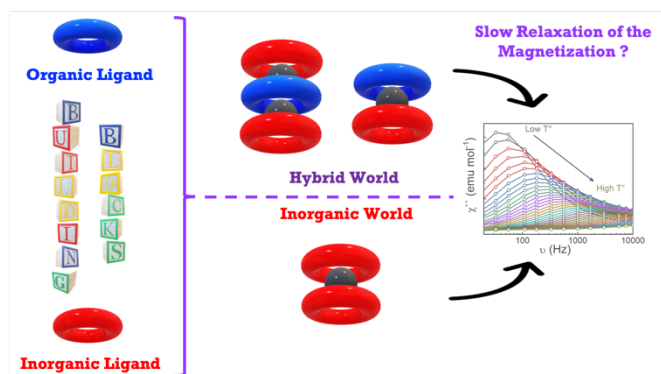
- [1] J.-P. Launay, M. Verdaguer, *Electrons in Molecules: From Basic Principles to Molecular Electronics*, Oxford University Press, **2013**.
- [2] J.-L. Liu, Y.-C. Chen, M.-L. Tong, *Chem. Soc. Rev.* **2018**, *47*, 2431–2453.
- [3] I. F. Díaz-Ortega, J. M. Herrera, Á. Reyes Carmona, J. R. Galán-Mascarós, S. Dey, H. Nojiri, G. Rajaraman, E. Colacio, *Front. Chem.* **2018**, *6*, 1–17.
- [4] Moeller T, *Adv. Chem.* **1967**, *62*, 306–317.
- [5] K. Liu, X. Zhang, X. Meng, W. Shi, P. Cheng, A. K. Powell, *Chem. Soc. Rev.* **2016**, *45*, 2423–2439.
- [6] N. Ishikawa, M. Sugita, T. Ishikawa, S. Y. Koshihara, Y. Kaizu, *J. Am. Chem. Soc.* **2003**, *125*, 8694–8695.
- [7] M. A. AlDamen, J. M. Clemente-Juan, E. Coronado, C. Martí-Gastaldo, A. Gaita-Ariño, *J. Am. Chem. Soc.* **2008**, *130*, 8874–8875.
- [8] S. Da Jiang, B. W. Wang, G. Su, Z. M. Wang, S. Gao, *Angew. Chem. Int. Ed.* **2010**, *49*, 7448–7451.

MINIREVIEW

- [9] S. Da Jiang, B. W. Wang, H. L. Sun, Z. M. Wang, S. Gao, *J. Am. Chem. Soc.* **2011**, *133*, 4730–4733.
- [10] D. N. Woodruff, R. E. P. Winpenny, R. A. Layfield, *Chem. Rev.* **2013**, *113*, 5110–5148.
- [11] R. Sessoli, *Nature* **2017**, *548*, 400–401.
- [12] D. Gatteschi, R. Sessoli, *Angew. Chem. Int. Ed.* **2003**, *42*, 268–297.
- [13] D. Gatteschi, R. Sessoli, J. Villain, *Molecular Nanomagnets*, Oxford University Press, **2006**.
- [14] M. Feng, M.-L. Tong, *Chem. - A Eur. J.* **2018**, *24*, 7574–7594.
- [15] F. Troiani, M. Affronte, *Chem. Soc. Rev.* **2011**, *40*, 3119–3129.
- [16] Y.-S. Ding, K.-X. Yu, D. Reta, F. Ortu, R. E. P. Winpenny, Y.-Z. Zheng, N. F. Chilton, *Nat. Commun.* **2018**, *9*, 3134.
- [17] Y.-N. Guo, G.-F. Xu, Y. Guo, J. Tang, *Dalton Trans.* **2011**, *40*, 9953.
- [18] S. Gómez-Coca, A. Urtizberea, E. Cremades, P. J. Alonso, A. Camón, E. Ruiz, F. Luis, *Nat. Commun.* **2014**, *5*, 4300.
- [19] J. Dreiser, *J. Phys. Condens. Matter* **2015**, *27*, 183203.
- [20] K. S. Pedersen, L. Ungur, M. Sigrist, A. Sundt, M. Schau-Magnussen, V. Vieru, H. Mutka, S. Rols, H. Weihe, O. Waldmann, L. F. Chibotaru, J. Bendix, J. Dreiser, *Chem. Sci.* **2014**, *5*, 1650–1660.
- [21] E. Lucaccini, L. Sorace, M. Perfetti, J.-P. Costes, R. Sessoli, *Chem. Commun.* **2014**, *50*, 1648–1651.
- [22] Y. S. Ding, N. F. Chilton, R. E. P. Winpenny, Y. Z. Zheng, *Angew. Chem. Int. Ed.* **2016**, *55*, 16071–16074.
- [23] R. Orbach, *Proc. R. Soc. A Math. Phys. Eng. Sci.* **1961**, *264*, 458–484.
- [24] K. N. Shrivastava, *Phys. Status Solidi* **1983**, *117*, 437–458.
- [25] J. Tang, P. Zhang, *Lanthanide Single Molecule Magnets*, Springer Berlin Heidelberg, Berlin, Heidelberg, **2015**.
- [26] Y. Rechkemmer, J. E. Fischer, R. Marx, M. Dörfel, P. Neugebauer, S. Horvath, M. Gysler, T. Brock-Nannestad, W. Frey, M. F. Reid, J. van Slageren, *J. Am. Chem. Soc.* **2015**, *137*, 13114–13120.
- [27] L.-F. Wang, J.-Z. Qiu, J.-L. Liu, Y.-C. Chen, J.-H. Jia, J. Jover, E. Ruiz, M.-L. Tong, *Chem. Commun.* **2015**, *51*, 15358–15361.
- [28] A. Lunghi, F. Totti, R. Sessoli, S. Sanvito, *Nat. Commun.* **2017**, *8*, 14620.
- [29] K. L. M. Harriman, D. Errulat, M. Murugesu, *Trends Chem.* **2019**, *1*, 425–439.
- [30] M. Mariani, F. Borsa, M. J. Graf, S. Sanna, M. Filibian, T. Orlando, K. P. V. Sabareesh, S. Cardona-Serra, E. Coronado, A. Lascialfari, *Phys. Rev. B* **2018**, *97*, 144414.
- [31] Y. F. Deng, T. Han, B. Yin, Y. Z. Zheng, *Inorg. Chem. Front.* **2017**, *4*, 1141–1148.
- [32] L. T. A. Ho, L. F. Chibotaru, *Phys. Rev. B* **2016**, *94*, 104422.
- [33] G.-J. Chen, C.-Y. Gao, J.-L. Tian, J. Tang, W. Gu, X. Liu, S.-P. Yan, D.-Z. Liao, P. Cheng, *Dalton Trans.* **2011**, *40*, 5579.
- [34] S. G. Miralles, A. Bedoya-Pinto, J. J. Baldoví, W. Cañón-Mancisidor, Y. Prado, H. Prima-García, A. Gaita-Ariño, G. Mínguez Espallargas, L. E. Hueso, E. Coronado, *Chem. Sci.* **2018**, *9*, 199–208.
- [35] W. Cañón-Mancisidor, S. G. Miralles, J. J. Baldoví, G. M. Espallargas, A. Gaita-Ariño, E. Coronado, *Inorg. Chem.* **2018**, *57*, 14170–14177.
- [36] J. Wu, J. Jung, P. Zhang, H. Zhang, J. Tang, B. Le Guennic, *Chem. Sci.* **2016**, *7*, 3632–3639.
- [37] S. Bala, G.-Z. Huang, Z.-Y. Ruan, S.-G. Wu, Y. Liu, L.-F. Wang, J.-L. Liu, M.-L. Tong, *Chem. Commun.* **2019**, *55*, 9939–9942.
- [38] D. Aravena, E. Ruiz, *Inorg. Chem.* **2013**, *52*, 13770–13778.
- [39] A. Dolbecq, E. Dumas, C. R. Mayer, P. Mialane, *Chem. Rev.* **2010**, *110*, 6009–6048.
- [40] P. Mialane, A. Dolbecq, E. Rivière, J. Marrot, F. Sécheresse, *Eur. J. Inorg. Chem.* **2004**, *2004*, 33–36.
- [41] M. T. Pope, in *Compr. Coord. Chem. II*, Elsevier: New York, NY, USA, **2004**, pp. 635–678.
- [42] R. Contant, W. G. Klempere, O. Yaghi, *Inorg. Synth.* **1990**, *27*, 104–111.
- [43] A. Tézé, G. Hervé, *Inorg. Synth.* **1990**, *27*, 85–96.
- [44] M. Vonci, C. Boskovic, *Aust. J. Chem.* **2014**, *67*, 1542–1552.
- [45] X. Ma, W. Yang, L. Chen, J. Zhao, *CrystEngComm* **2015**, *17*, 8175–8197.
- [46] M. Ibrahim, I. M. Mbomekallé, P. de Oliveira, A. Baksi, A. B. Carter, Y. Peng, T. Bergfeldt, S. Malik, C. E. Anson, *ACS Omega* **2019**, *4*, 21873–21882.
- [47] M. A. AlDamen, S. Cardona-Serra, J. M. Clemente-Juan, E. Coronado, A. Gaita-Ariño, C. Martí-Gastaldo, F. Luis, O. Montero, *Inorg. Chem.* **2009**, *48*, 3467–3479.
- [48] P. Ma, F. Hu, R. Wan, Y. Huo, D. Zhang, J. Niu, J. Wang, *J. Mater. Chem. C* **2016**, *4*, 5424–5433.
- [49] J. Niu, K. Wang, H. Chen, J. Zhao, P. Ma, J. Wang, M. Li, Y. Bai, D. Dang, *Cryst. Growth Des.* **2009**, *9*, 4362–4372.
- [50] S. Zhang, Y. Wang, J. Zhao, P. Ma, J. Wang, J. Niu, *Dalton Trans.* **2012**, *41*, 3764–3772.
- [51] P. Ma, R. Wan, Y. Si, F. Hu, Y. Wang, J. Niu, J. Wang, *Dalton Trans.* **2015**, *44*, 11514–11523.
- [52] W. Cañón-Mancisidor, M. Zapata-Lizama, P. Hermosilla-Ibáñez, C. Cruz, D. Venegas-Yazigi, G. Mínguez Espallargas, *Chem. Commun.* **2019**, *55*, 14992–14995.
- [53] S. Sarwar, S. Sanz, J. van Leusen, G. S. Nichol, E. K. Brechin, P. Kögerler, *Dalton Trans.* **2020**, *49*, 16638–16642.
- [54] M. Arab Fashapoyeh, M. Mirzaei, H. Eshtiagh-Hosseini, A. Rajagopal, M. Lechner, R. Liu, C. Streb, *Chem. Commun.* **2018**, *54*, 10427–10430.
- [55] A. S. Mougharbel, S. Bhattacharya, B. S. Bassil, A. Rubab, J. van Leusen, P. Kögerler, J. Wojciechowski, U. Kortz, *Inorg. Chem.* **2020**, *59*, 4340–4348.
- [56] B. S. Bassil, M. H. Dickman, B. von der Kammer, U. Kortz, *Inorg. Chem.* **2007**, *46*, 2452–2458.
- [57] J. Iijima, H. Naruke, T. Sanji, *RSC Adv.* **2016**, *6*, 91494–91507.
- [58] P. Ma, F. Hu, Y. Huo, D. Zhang, C. Zhang, J. Niu, J. Wang, *Cryst. Growth Des.* **2017**, *17*, 1947–1956.
- [59] E. Radkov, R. H. Beer, *Polyhedron* **1995**, *14*, 2139–2143.
- [60] D. Zhang, C. Zhang, H. Chen, P. Ma, J. Wang, J. Niu, *Inorg. Chim. Acta* **2012**, *391*, 218–223.
- [61] M. K. Saini, R. Gupta, S. Parbhakar, A. Kumar Mishra, R. Mathur, F. Hussain, *RSC Adv.* **2014**, *4*, 25357–25364.
- [62] F. Hussain, S. Sandriesser, M. Speldrich, G. R. Patzke, *J. Solid State Chem.* **2011**, *184*, 214–219.
- [63] L. Xiao, T.-T. Zhang, Z. Liu, X. Shi, H. Zhang, L. Yin, L.-Y. Yao, C.-C. Xing, X.-B. Cui, *Inorg. Chem. Commun.* **2018**, *95*, 86–89.
- [64] D. Casanova, J. Cirera, M. Llunell, P. Alemany, D. Avnir, S. Alvarez, *J. Am. Chem. Soc.* **2004**, *126*, 1755–1763.
- [65] D. Casanova, P. Alemany, J. M. Bofill, S. Alvarez, *Chem. - A Eur. J.* **2003**, *9*, 1281–1295.
- [66] D. Casanova, M. Llunell, P. Alemany, S. Álvarez, *Chem. - A Eur. J.* **2005**, *11*, 1479–1494.
- [67] J. W. Zhao, Y. Z. Li, L. J. Chen, G. Y. Yang, *Chem. Commun.* **2016**, *52*, 4418–4445.
- [68] M. Zapata-Lizama, P. Hermosilla-Ibáñez, D. Venegas-Yazigi, G. Mínguez Espallargas, L. J. Queiroz Maia, G. Gasparotto, R. C. De Santana, W. Cañón-Mancisidor, *Inorg. Chem. Front.* **2020**, *7*, 3049–3062.
- [69] J.-P. Wang, X.-Y. Duan, X.-D. Du, J.-Y. Niu, *Cryst. Growth Des.* **2006**, *6*, 2266–2270.
- [70] Y. Huo, Y.-C. Chen, S.-G. Wu, J.-L. Liu, J.-H. Jia, W.-B. Chen, B.-L. Wang, Y.-Q. Zhang, M.-L. Tong, *Inorg. Chem.* **2019**, *58*, 1301–1308.
- [71] Y. Li, Y. Liu, P. Gong, X. Tian, J. Luo, J. Zhao, *Inorg. Chem. Commun.* **2016**, *74*, 42–47.
- [72] Q. Zhou, F. Yang, D. Liu, Y. Peng, G. Li, Z. Shi, S. Feng, *Inorg. Chem.* **2012**, *51*, 7529–7536.
- [73] H.-S. Wang, K. Zhang, Y. Song, Z.-Q. Pan, *Inorg. Chim. Acta* **2021**, *521*, 120318.
- [74] J. P. Costes, S. Totos-Padilla, I. Oyarzabal, T. Gupta, C. Duhayon, G. Rajaraman, E. Colacio, *Inorg. Chem.* **2016**, *55*, 4428–4440.

MINIREVIEW

Entry for the Table of Contents



This mini review provides a comprehensive overview of the synthetic approach, structural analysis, and magnetic properties of Dy^{III}, Er^{III} and Yb^{III} inorganic and hybrid complexes. The structural analysis reflects that the nature of the heteroatom of the inorganic ligand can induce changes in the geometry of the Ln^{III} ion, and therefore, affects the magnetic properties of the system.

Twitter: @CanonMancisor